UDC 534.232.082.73

Mathematical Modelling of Disk Piezoelectric Transducers for Acoustoelectronic Devices

Bazilo C. V., Bondarenko M. O., Usyk L. M., Faure E. V., Kovalenko Yu. I.

Cherkasy State Technological University, Cherkasy, Ukraine

E-mail: *maxxium23@gmail.com*

This study has presented an algorithm for assembling, solving, and analyzing the results obtained by mathematical modeling of the disc piezoelectric transducers, which are widely used in hydroacoustics, microelectronics, microcircuit engineering (for example, as components of receiving antennas of hydroacoustic communication devices). The models developed in this study enable us to establish dependencies, which represent a mathematical description of the electroacoustic connection between the wave fields in different sections of the disc piezoelectric transducers. Analytical dependences obtained by mathematical modelling make it possible to establish the electrical impedance and quality factor together with the amplitude values of the electric charge and current on the electroded surfaces of the piezoelectric disk, subject to the inverse piezoelectric effect conditions. A complete calculation of the problem of harmonic radial oscillations of disc piezoelectric transducers allowed the authors to significantly expand the list of physical and mechanical parameters of the piezoelectric material, which had been previously determined experimentally. The research has revealed the dependence of the change in electrical impedance on the values of the electromechanical coupling coefficient, the wave number of elastic oscillations, and the Voigt indices. The study has also determined a high agreement between the electric impedance modules of discs made of lead zirconate titanate PZT piezoelectric ceramics with and without the piezoelectric effect (the difference between the impedance values in these cases did not exceed 18%).

Keywords: piezoelectric transducer; acoustoelectronics; mathematical mode; impedance; disk element

DOI: 10.20535/RADAP.2023.91.37-45

Introduction

Piezoelectric components and equipment designed with piezoelectric components have found multiple applications in modern science and technology [1]. Indeed, literally every research and technology field benefits from applying piezoelectric transducers nowadays. This fact is due to their high accuracy, reliability, manufacturability, multifunctionality, as well as their ability to miniaturize and integrate with various microelectronic and micromechanical components.

Energy independence from external sources may become an absolute advantage of piezoelectric components in the near future. Moreover, in some cases, piezoelectric components, when being an element of a device, can generate electric current for other electronic components of the same device [2].

At the same time, having analyzed the market of modern piezoelectric transducers (according to marketing research of the companies taking the lead in manufacturing piezoelectric components intended for various purposes, such as: Zhejiang Jiakang Electronics Co., Changzhou Keliking Electronics Co., PI Ceramic GmbH and others [3, 4]) we have established that a considerable share (about 56%) of the entire variety of form factors of piezoelectric transducers is accounted for disc piezoelectric transducers. This share amounts to nearly 615 million US dollars as of the third quarter of 2022.

However, further developments in the technological base of piezoelectric transducers with introducing expanded functional capabilities would not be possible without strengthening the scientific and theoretical foundations of piezoelectric technology by improving methodical, technological, and mathematical support.

Improvements in the mathematical support that underlies the piezoelectric transducers development theory, followed by their applied implementation as ready-made components, offer new methods to calculate, design and model disk-shaped piezoelectric transducers [5].

1 Relevance of the research based on the publication analysis results

Disk piezoelectric transducers serve as sound-receiving and sound-radiating devices, various sensors, and as components of receiving antennas in hydroacoustic communication devices [6, 7]. As indicated in the studies [8, 9], the standard design of piezoelectric stack transducers, as a rule, involves compiling disk elements into a single design, which expands the functional properties of such type of multi-array transducers, hence improving the operational properties of devices where these transducers are used. The study [8] presents findings related to the functional features of a new three-layer circular piezoelectric transducer, and first introduces an analytical model containing closed-form equations, which are important tools for predicting and optimizing the transducer's operation. Employing hence both the plate theory and the constitutive equations of piezoelectric materials, an analytical formula was found to describe the deflection of the transducer as a function of electrical loads (electromechanical characteristics of the transducer). The authors have conducted verification tests to demonstrate that the results obtained with the developed solution correspond satisfactorily to both literature and numerical data. Based on the obtained analytical model, the influence of selected dimensionless variables on the transducer's performance has been investigated. It has been demonstrated that parameters including the dimensions and mechanical properties of the piezoelectric disc significantly affect the transducer's performance. In addition, the authors of the study [9] discuss the results of investigating piezoelectric stack transducers connected in varied sequences. Designing and developing piezoelectric matrix options were implemented for series, parallel, series-parallel, and parallel-series connections of piezoelectric transducers. Modeling these options and analyzing the obtained results were conducted with the electronic circuit simulation software package PSIM. Verification of the simulation results has confirmed the feasibility to determine such operating modes of the piezoelectric matrix that provide the optimal output power, which can satisfy the minimum energy requirement for powering the device with the considered variant of the configuration of piezoelectric components with low load.

A number of surveys, namely those conducted by C. Bazilo, O. Petrishchev, I. Yanchevskiy, A. Zagorskis and others, focus on theoretical and applied research of piezoelectric technology and investigate the physical processes that occur in disk piezoelectric transducers with differently shaped electrodes [10–12]. For example, in the study [10], piezoelectric sensors for environmental monitoring are modeled and investigated. This analysis proves the absence of reliable and well-founded methods to build mathematical models of disc piezoelectric transducers, which could be used as a theoretical basis for calculating the characteristics and parameters of this class of functional components used in modern piezoelectric electronics. Analysis and further COMSOL Multiphysics software platform modeling of the physical processes that occur in piezoelectric transducers have established a significant expansion of the range of their mechanical characteristics and an increase in sensitivity when using these transducers in environmental monitoring tasks. Surveys such as [11, 12] undertake research of electromechanical and energy characteristics of piezoceramic elements during radial movements, which occur when their operating frequencies are close to resonance/anti-resonance values.

At the same time, the studies [13, 14] that focus on the possibility of modeling variously shaped piezoelectric transducers using equivalent circuits have demonstrated that it is impossible to consider mechanical processes and phenomena in piezoceramics, while establishing a connection between these processes and the electromechanical characteristics of piezoceramic material is complicated.

Thus, having analyzed the above-mentioned scientific publications, along with a number of publications [15–18] dedicated to the mathematical description of physical processes in piezoelectric disc transducers, the authors of this article established the absence of unified mathematical models of piezoelectric disc actuators. Any clear sequence of calculating their technical and operational characteristics is also absent.

Therefore, we consider development of a mathematical model of piezoelectric disc transducers and experimental confirmation of the results obtained with the help of the developed models as a topical problem, the solution of which is the main goal of this research.

2 Problem statement for modelling of a thin piezoceramic disk in the mode of thickness oscillations

Figure 1 demonstrates a disc with PZT-type piezoceramics polarized in direction Ox_3. Its surfaces $x_3=0$; $x_3=-\alpha$ are metallized [19]. The surface $x_3=-\alpha$ has zero potential, and the potential $\Phi(t) = U_0 e^{i\omega t}$ is supplied to the surface $x_3 = 0$ from an external generator, where U_0 is the voltage amplitude; $i = \sqrt{-1}$; ω is the circular frequency of the charge sign reversal in the electric potential; t is time.

We consider the disk sufficiently thin, i.e., the strong inequality $\alpha/R \ll 1$ takes place. Apart from that, we consider that the disk is isolated from any mechanical contacts with other material objects. For definiteness, we assume that the disk is in vacuum.

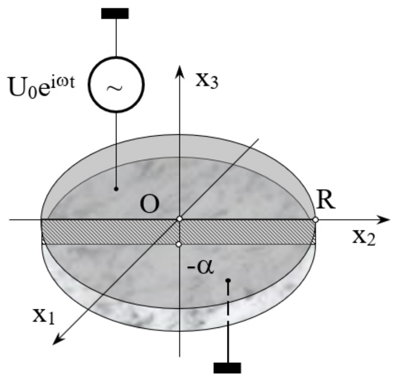

Fig. 1. Calculation scheme of a piezoceramic disk

The action of an externally applied electric potential difference induces an external electric field in the disk, which acts on the piezoceramic ions through the Coulomb forces, which means that an inverse piezoelectric effect appears in the volume of the disk. Here we assume that the frequency ω is such that the spatial inhomogeneity scale of the stress-strain state in the disk is commensurate with its thickness. Since the inequality $\alpha/R \ll 1$ is satisfied, one can safely neglect the influence of the lateral disk boundary on the characteristics and parameters of its stress-strain state and consider that the displacement vector $\vec{u}\,(x_k)$ of the material particles in the piezoceramics is determined on average by the axial component u_3. If we take into consideration that the component u_3 solely depends on the coordinate x_3, then the real stress-strain state of the disk is reduced to a uniaxial deformed state. A uniaxial deformed state is a stress-strain state of an elastic body in which the strain tensor has only one nonzero component. In the model situation formulated above, such a component is the quantity $\varepsilon_{33} = \partial u_3/\partial x_3$. The two components that define compression and tension along the axes Ox$_1$ and Ox$_2$, that is, along the radial and circumferential axes of the cylindrical coordinate system, are equal to zero.

Under the above conditions, the electrical impedance $Z_{el}(\omega)$ of a disk oscillating through its thickness should be determined.

3 Construction of a mathematical model of thin piezoceramic disk in the mode of thickness oscillations

As a rule [20], qualitative and quantitative parameters of the stress-strain state of an oscillating piezoceramic element are determined before calculating the electric current in the conductor that connects the disk's electroded surface to the electric potential generator (Fig. 1). To perform these estimates, we note the generalized Hooke's law in the inverse formulation [21]

$$\varepsilon_{ij} = s^E_{ijkl}\sigma_{kl} + d_{kij}E_k, \tag{1}$$

which we obtain from the Taylor's expansions of the functions ε_{ij}, D_m and S, with independent variables σ_{kl}, E_k and T. The symbol s^E_{ijkl} in expression (1) denotes the component of the piezoceramics' elastic compliance tensor. The symbol d_{kij} denotes the piezoelectric charge modulus. There exist clearly defined relations between the s^E_{ijkl} and d_{kij} values, as well as between the elastic moduli c^E_{ijkl} and the piezoelectric moduli e_{kij}. These relations shall be noted as follows

$$c^E_{\alpha\beta}s^E_{\beta\gamma} = \delta_{\alpha\gamma}, \quad d_{k\beta} = e_{k\alpha}s^E_{\alpha\beta}, \tag{2}$$

where α, β, γ are Voigt indices; $\delta_{\alpha\gamma}$ is the Kronecker symbol.

From relation (1) it follows that

$$\varepsilon_1 = s^E_{11}\sigma_1 + s^E_{12}\sigma_2 + s^E_{13}\sigma_3 + d_{31}E_3 = 0, \tag{3}$$

$$\varepsilon_2 = s^E_{21}\sigma_1 + s^E_{22}\sigma_2 + s^E_{23}\sigma_3 + d_{32}E_3 = 0, \tag{4}$$

$$\varepsilon_3 = s^E_{31}\sigma_1 + s^E_{32}\sigma_2 + s^E_{33}\sigma_3 + d_{33}E_3 \neq 0. \tag{5}$$

In relations (3)–(5), the notation with Voigt indices is used for the components of strain and stress tensors. Shear deformations ε_β ($\beta = 4$, 5, 6) due to the physical content of the problem identification are equal to zero.

Since matrices $s^E_{\alpha\beta}$ and $d_{k\alpha}$ are similar to matrices $c^E_{\alpha\beta}$ and e_k in their structure and the relations between the matrices' elements, it follows that $d_{31} = d_{32}$. In this case, it follows from equations (3) and (4) that

$$\sigma_1 = \sigma_2 = -\frac{d_{31}}{s^E_{11} + s^E_{12}}E_3 - \frac{s^E_{13}}{s^E_{11} + s^E_{12}}\sigma_3. \tag{6}$$

Substituting the stresses σ_1 and σ_2 determined by expression (6) into relation (5), we obtain the notation

$$\varepsilon_3 = \frac{\sigma_3}{M^E} + \left[d_{33} - 2\frac{s^E_{13}d_{31}}{s^E_{11} + s^E_{12}}\right]E_3, \tag{7}$$

where M^E is the elastic modulus for the uniaxial deformed state mode (compression – tension through the thickness) of the disk. Wherein

$$\frac{1}{M^E} = s^E_{33} - \frac{2\left(s^E_{13}\right)^2}{s^E_{11} + s^E_{12}}. \tag{8}$$

Generally, we can note the Hooke's law (7) as follows

$$\sigma_3 = M^E\varepsilon_3 - e_{(\varepsilon)}E_3, \tag{9}$$

where

$$e_{(\varepsilon)} = \left[d_{33} - 2\frac{s^E_{13}d_{31}}{s^E_{11} + s^E_{12}}\right]M^E. \tag{10}$$

We assign the value $e_{(\eta)}$ to represent the piezoelectric modulus for the mode of uniaxial compression – tension of the disk.

Here we determine the quantities M^E and $e_{(\eta)}$ through the elastic moduli $c^E_{\alpha\beta}$ and the piezoelectric modules $e_{k\alpha}$.

The elastic moduli $c^E_{\alpha\beta}$ matrix for a polarized through the thickness PZT-piezoceramic plate is noted as follows

$$\left|c^E_{\alpha\beta}\right| = \begin{vmatrix} c^E_{11} & c^E_{12} & c^E_{13} & 0 & 0 & 0 \\ & c^E_{22} & c^E_{23} & 0 & 0 & 0 \\ & & c^E_{33} & 0 & 0 & 0 \\ & & & c^E_{44} & 0 & 0 \\ & & & & c^E_{55} & 0 \\ & & & & & c^E_{66} \end{vmatrix}, \quad (11)$$

where $c^E_{11} = c^E_{22}$; $c^E_{13} = c^E_{23}$ and $c^E_{44} = c^E_{55}$.

The elements of the elastic compliance matrix $s^E_{\lambda\mu}$ are calculated from the elements $c^E_{\alpha\beta}$ of the elastic moduli matrix in the following notation

$$s^E_{\lambda\mu} = (-1)^{\lambda+\mu} \frac{M_{\lambda\mu}}{\Delta_0}, \quad (12)$$

where $M_{\lambda\mu}$ is the algebraic cofactor at the element $c^E_{\lambda\mu}$ that is located at the crosshairs of the λ-th row and the μ-th column; $\Delta_0 = c^E_{11}\left[c^E_{11}c^E_{33} - 2\left(c^E_{13}\right)^2\right] - c^E_{12}\left[c^E_{12}c^E_{33} - 2\left(c^E_{13}\right)^2\right]$ defines the matrix (11).

The elastic compliances included into the definitions of M^E and $e_{(\eta)}$ are determined in accordance with expression (12) as follows

$$\begin{aligned} s^E_{11} &= \left[c^E_{11}c^E_{33} - \left(c^E_{13}\right)^2\right]/\Delta_0; \\ s^E_{12} &= -\left[c^E_{12}c^E_{33} - \left(c^E_{13}\right)^2\right]/\Delta_0; \\ s^E_{13} &= \left[c^E_{12}c^E_{13} - c^E_{13}c^E_{11}\right]/\Delta_0; \\ s^E_{33} &= \left[\left(c^E_{11}\right)^2 - \left(c^E_{13}\right)^2\right]/\Delta_0. \end{aligned} \quad (13)$$

Substituting relations (13) into the definition (8) of the elastic modulus M^E results in the following relation

$$M^E = \frac{c^E_{33}\Delta_0}{\left(c^E_{11} - c^E_{12}\right)\left[c^E_{33}\left(c^E_{11} + c^E_{12}\right) - 2\left(c^E_{13}\right)^2\right]}. \quad (14)$$

According to the expression (2), the piezoelectric moduli d_{31} and d_{33} are defined by the following relations

$$\begin{aligned} d_{31} &= e_{3\alpha}s^E_{\alpha 1} = e_{31}\left(s^E_{11} + s^E_{21}\right) + e_{33}s^E_{31}; \\ d_{33} &= e_{3\alpha}s^E_{\alpha 3} = e_{31}\left(s^E_{13} + s^E_{23}\right) + e_{33}s^E_{33}. \end{aligned} \quad (15)$$

When noting the relations (15), we considered the notation of the piezoelectric moduli matrix $e_{k\alpha}$

$$\left|e_{k\alpha}\right| = \begin{vmatrix} 0 & 0 & 0 & 0 & e_{15} & 0 \\ 0 & 0 & 0 & e_{24} & 0 & 0 \\ e_{31} & e_{32} & e_{33} & 0 & 0 & 0 \end{vmatrix}, \quad (16)$$

where $e_{31} = e_{32}$ and $e_{15} = e_{24}$.

Substituting expressions (13), (14) and (15) into the definition (10) of the piezoelectric modulus $e_{(\eta)}$ we come to the conclusion that $e_{(\eta)} = e_{33}$. If we assume that $c^E_{12} = c^E_{13}$ (a transversely isotropic elastic medium), from expression (14) it follows that $M^E = c^E_{33}$.

Thus, under uniaxial compression – tension of a polarized through thickness piezoceramic plate (disk) with the elastic properties of a transversally isotropic solid ($c^E_{12} = c^E_{13}$), the following notation of the generalized Hooke's law can be used

$$\sigma_3 = c^E_{33}\varepsilon_3 - e_{33}E_3. \quad (17)$$

In order to determine the resulting electric field strength E_3 that we have in the relation (17), we consider the condition when free electricity carriers are absent in the volume of the deformable piezoceramic. For the case under consideration, we obtain $\partial D_3/\partial x_3 = 0$ from the general formulation of this condition $div\,\vec{D} = 0$, where $D_3 = e_{33}\varepsilon_3 + \chi^\varepsilon_{33}E_3$. Since $\varepsilon_3 = \partial u_3/\partial x_3$ and $E_3 = -\partial\Phi/\partial x_3$, where Φ is the electric potential of the resulting field within the volume of the deformable piezoelectric, we note the expression for the vertical component of the electric induction vector

$$D_3 = e_{33}\frac{\partial u_3}{\partial x_3} - \chi^\varepsilon_{33}\frac{\partial\Phi}{\partial x_3}, \quad (18)$$

where D_3, u_3 and Φ are amplitude values of harmonically time-varying quantities.

The vertical component D_3 of the electric induction vector does not depend on the values of the coordinate x_3. Therefore, by integrating the left and the right parts of relation (18) with respect to the variable x_3 within the range from $-\alpha$ to 0, we obtain

$$D_3 = \frac{e_{33}}{\alpha}\left[u_3(0) - u_3(-\alpha)\right] - \frac{\chi^\varepsilon_{33}}{\alpha}\left[\Phi(0) - \Phi(-\alpha)\right]. \quad (19)$$

Obviously, the closing square bracket in the formula (19) is equal to the amplitude of the electric potential U_0 (Fig. 1) supplied to the electroded surface $x_3 = 0$ from an electrical signal generator. Therefore

$$D_3 = \frac{e_{33}}{\alpha}\left[u_3(0) - u_3(-\alpha)\right] - \frac{\chi^\varepsilon_{33}}{\alpha}U_0. \quad (20)$$

By substituting the right side of the expression (20) into the left side of the above definition of the quantity D_3 we obtain

$$e_{33}\frac{\partial u_3}{\partial x_3} + \chi^\varepsilon_{33}E_3 = \frac{e_{33}}{\alpha}\left[u_3(0) - u_3(-\alpha)\right] - \frac{\chi^\varepsilon_{33}}{\alpha}U_0,$$

whence it follows that

$$E_3 = -\frac{e_{33}}{\chi^\varepsilon_{33}}\frac{\partial u_3}{\partial x_3} + \frac{e_{33}}{\alpha\chi^\varepsilon_{33}}\left[u_3(0) - u_3(-\alpha)\right] - \frac{U_0}{\alpha}. \quad (21)$$

In the formula (21) for calculating the vertical component of the resulting electric field strength vector, the first two terms determine the internal electric field that arises in the volume of the deformable piezoceramic due to the ions being displaced from the equilibrium position. The third term determines the strength of the electric field created by an external source, that is, the electrical signal generator.

Substituting the relation (21) into the generalized Hooke's law (17) produces

$$\sigma_3 = c_{33}^D \frac{\partial u_3}{\partial x_3} - \frac{e_{33}^2}{\alpha \chi_{33}^\varepsilon} \left[u_3(0) - u_3(-\alpha)\right] + \frac{e_{33}}{\alpha} U_0, \quad (22)$$

where $c_{33}^D = c_{33}^E \left(1 + K_3^2\right)$ is the elasticity modulus in the mode of electric induction constancy (equal to zero); $K_3^2 = e_{33}^2 / \left(\chi_{33}^\varepsilon c_{33}^E\right)$ is squared electromechanical coupling coefficient in the mode of thickness oscillations in a polarized through thickness piezoceramic disk. For PZT-type piezoceramics, its value is $K_3^2 \leq 0,5$. The elasticity modulus c_{33}^D counts in the consistent (coherent) action of elastic forces and Coulomb forces in the volume of the deformable piezoelectric. Therefore, $c_{33}^D > c_{33}^E$.

The amplitudes of both the stress tensor σ_3 and the displacement vector u_3 components that vary harmonically in time must satisfy Newton's second law in differential form, which, as applied to the situation under consideration, is a notation

$$\frac{\partial \sigma_3}{\partial x_3} + \rho_0 \omega^2 u_3 = 0 \, \forall x_k \in V, \quad (23)$$

where ρ_0 is density; V denotes the volume of the piezoceramic disc.

By substituting the definition (22) of the resulting voltage σ_3 into the equation (23) we compose

$$\frac{\partial^2 u_3}{\partial x_3^2} + \gamma^2 u_3 = 0 \, \forall x_k \in V, \quad (24)$$

where $\gamma = \omega / \sqrt{c_{33}^D / \rho_0}$ is the wave number of elastic vibrations in the volume of the piezoceramic disk.

Indeed, the solution of the equation (24) is

$$u_3 = A \cos \gamma x_3 + B \sin \gamma x_3, \quad (25)$$

where A and B are the constants to be defined from the boundary conditions, which in their physical essence represent Newton's third law in differential form.

With regard to the problem being solved, it then follows that

$$\sigma_3|_{x_3 = (0, -\alpha)} = 0 \, \forall x_k \in S, \quad (26)$$

where S denotes the metallized surfaces $x_3 = (0\,;\,-\alpha)$ (Fig. 1) of the oscillating disk.

Let expression (25) for calculating the amplitude of the displacement vector's vertical component u_3 be substituted into the definition (22) of the stress tensor component σ_3 amplitude harmonically varying in time. In the result obtained, we equate the coordinate value to zero first, and then assign $x_3 = -\alpha$, we equate the expressions obtained to zero, as required by condition (26). In this case we obtain a system of two algebraic equations that contain the two required coefficients, A and B.

The indicated system of equations is solved with respect to the required coefficients A and B in a unique way. The final result of solving this system of equations is the notation

$$A = -\frac{e_{33} U_0}{c_{33}^D \Lambda} \cdot \frac{(1 - \cos \gamma\alpha)}{\gamma\alpha}; \qquad B = -\frac{e_{33} U_0}{c_{33}^D \Lambda} \cdot \frac{\sin \gamma\alpha}{\gamma\alpha}, \quad (27)$$

where $\Lambda = \sin \gamma\alpha \left[1 - \frac{K_3^2}{1 + K_3^2} \cdot \frac{tg(\gamma\alpha/2)}{(\gamma\alpha/2)}\right] = \sin \gamma\alpha \cdot \Lambda_0$.

It then follows that the amplitudes of the harmonically time-varying displacements u_3 of the piezoceramic disk's material particles, which satisfy the fundamental laws of mechanics, i.e., Newton's second and third laws, are to be determined by the following expression

$$u_3 = -\frac{e_{33} U_0}{c_{33}^D \Lambda} \left[\frac{(1 - \cos \gamma\alpha)}{\gamma\alpha} \cos \gamma x_3 + \frac{\sin \gamma\alpha}{\gamma\alpha} \sin \gamma x_3\right]. \quad (28)$$

Substituting expression (28) into definition (20) of the vertical componentwe obtain

$$D_3 = -\frac{\chi_{33}^\varepsilon U_0}{\alpha \Lambda_0},$$

where $\Lambda_0 = 1 - \frac{K_3^2}{1 + K_3^2} \cdot \frac{tg(\gamma\alpha/2)}{(\gamma\alpha/2)}$.

The amplitude value I_0 of the electric current harmonically changing in time within the conductors is determined through the value D_3

$$I_0 = -i\omega S D_3 = i\omega C_0^\varepsilon \frac{U_0}{\Lambda_0}, \quad (29)$$

where $C_0^\varepsilon = S \chi_{33}^\varepsilon / \alpha$ is the dynamic electrical capacitance of the electroded piezoceramic disc.

The formula below defines the electrical impedance $Z_{el}(\omega)$ of an oscillating piezoceramic disk by Ohm's law for a section of an electrical circuit

$$Z_{el}(\omega) = \frac{U_0}{I_0} = \frac{1}{i\omega C_0^\varepsilon} \Lambda_0. \quad (30)$$

Next, we consider the physical content of the results obtained.

If the dielectric placed between the electroded surfaces does not possess piezoelectric properties, then $K_3^2 = 0$ and $\Lambda_0 = 1$. The expression (30) acquires the meaning of a formula widely used in electrical engineering to calculate the electric capacitance reactance of a flat capacitor. When $K_3^2 \neq 0$, the frequency-dependent change in the electrical impedance $Z_{el}(\omega)$ becomes much more complicated due to alterations introduced to the function Λ_0.

Figure 2 contains a graph reflecting the dynamics of the Λ_0 function calculated for $K_3^2 = 0,5$. With $\gamma\alpha \to 0$, we have $\Lambda_0 = 1/\left(1 + K_3^2\right)$. As the argument $\gamma\alpha$ increases, the tangent also increases and for a definite frequency, which is marked with symbol ω_r in Figure 2, the function becomes $\Lambda_0 = 0$. It then follows at once that $Z_{el}(\omega_r) = 0$. At a frequency of ω_r, when $\Lambda_0 = 0$, the displacement amplitudes of the piezoceramic disk material particles increase indefinitely. This phenomenon is caused by the material particles being displaced within the volume of the deformable disk that generate an internal electric field, the direction of which coincides with the external electric field. In other words, the internal electric field complements the external electric field, hence the strength of the resulting electric field increases. This leads to an increase in the displacement amplitudes of the piezoceramic material particles. In its turn, the strength of the resulting electric field increases again, and so do the displacement amplitudes of the material particles. In the case when an ideal generator of a harmonically time-varying electric potential difference is present, the displacement amplitudes of material particles in an ideal (without loss of elastic vibrations energy) piezoelectric increase indefinitely at ω_p frequency. In this case, infinitely large polarization charges are produced and electric currents of infinitely large amplitude flow through the conductors. The described situation corresponds to the short circuit mode, i.e., a $Z_{el}(\omega_r) = 0$ condition in the circuit of an ideal electric potential difference generator. Naturally, the electrical load, that is, the oscillating piezoceramic disk, consumes the maximum possible amount of energy from the electrical signal generator in this case. The physical state of any system that operates on the energy produced by an external source, in which the system consumes the maximum possible amount of energy from the source, is called resonance. For this reason, ω_r frequency is called the resonance frequency, and the physical state of the oscillating disk is called the electromechanical resonance [22].

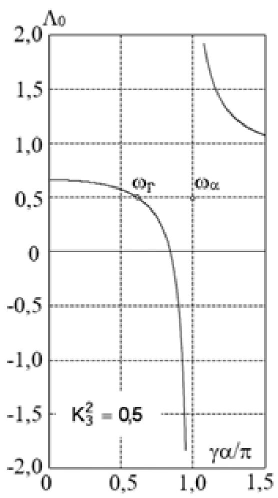

Fig. 2. Frequency graph for the Λ_0 function

In a real-life situation, currents of finite amplitude flow along the conductors of the electrical circuit, which is shown in Figure 1. We can define two factors causing this effect. First, an electrical signal generator has a finite internal resistance R_r, while an ideal electrical voltage generator has zero resistance. Secondly, the piezoceramic material absorbs the energy of elastic vibrations and converts it into heat.

The integral estimate of energy losses in the volume of a dynamically deformed solid is a dimensionless quantity Q_0, which is called the quality factor. The numerical value of the Q_0 parameter is inversely proportional to the amount of energy loss in the material during the sign inversion of the stress-strain state. In this case, the wave number γ becomes a complex-valued function of the frequency and is determined as follows: $\gamma = \gamma_0\,(1 - i/(2Q_0))$, where $\gamma_0 = \omega/\sqrt{{}^0c_{33}^D/\rho_0}$; ${}^0c_{33}^D$ is the static modulus of elasticity. The complex number γ transforms the function Λ into a category of a complex variable function, which at ω_r frequency has a non-zero finite value. In this case, the electrical impedance of the oscillating disk acquires Z_0 value, which is an active resistance by its content. This statement has been fully confirmed by the experimentally observed facts.

If the symbol ε denotes the value $1/(2Q_0)$, which is obviously a small parameter, then the expansion of the function Λ_0 in a power series with respect to the small parameter ε with an accuracy of ε^2 and higher orders of magnitude produces the following expression for the electrical impedance at the frequency of the first electromechanical resonance

$$Z_{el}\,(\omega_p) = Z_0 = \frac{K_3^2}{2\,(1+K_3^2)\,Q_0\omega_p C_0^\varepsilon} \cdot \frac{[x_p - \sin x_p \cos x_p]}{x_p \cos^2 x_p},$$

where $x_p = \omega_p\alpha \Big/ \left(2\sqrt{{}^0c_{33}^D/\rho_0}\right)$.

The latter relation defines the numerical value of the piezoceramics' quality factor at the frequency of the first electromechanical resonance

$$Q_0 = \frac{K_3^2}{2\,(1+K_3^2)\,Z_0\omega_p C_0^\varepsilon} \cdot \frac{[x_p - \sin x_p \cos x_p]}{x_p \cos^2 x_p}. \qquad (31)$$

For PZT-type piezoceramics, the quality factor Q_0 has a value of 100…200 relative units at frequencies (1…2) MHz.

At the frequency ω_α, when $\gamma\alpha/2 = \pi/2$, the function Λ_0 tends to infinity, accordingly, $|Z_{el}(\omega_\alpha)| \to \infty$. In this case, the amplitude of the electric current in the conductors of the electrical circuit (Fig. 1) tends to zero. The piezoelectric disk ceases to consume energy from the source, i.e., from the generator of the electrical potential difference. Hence ω_α is called the frequency of electromechanical antiresonance. The physical essence of electromechanical antiresonance lies in the fact that the polarization charge in the volume of the oscillating disk completely compensates for the electric charge induced by the electric potential difference generator on the electroded surfaces of the piezoceramic disk. Electromechanical antiresonance is the result of the algebraic addition of the polarization charge and the electric charge induced by the generator. If there is no external generator of electric potential difference, the electromechanical antiresonance is not observed. This is a typical situation in the case of using piezoelectric elements as an elastic vibrations receiver. In a real-life situation, the electrical impedance of the piezoceramic disk at ω_α frequency exceeds the electrical impedance Z_0 at ω_r frequency by almost three orders of magnitude.

4 Discussion and experimental confirmation of simulation results

Figure 3 shows the electrical impedance modulus of a PZT–19 piezoceramic disc. The disc's material parameters are c_{33}^E=106 GPa; ρ_0=7400 kg/m^3; e_{33}=18 C/m^2; $\chi_{33}^\varepsilon = 1000\chi_0$; χ_0=8.85·10^{-12} F/m; the ceramics quality factor is Q_0=100. The radius R of the disk exceeds the thickness α of the disk ten times (R/α=10). The electrical impedance modulus values in ohms are plotted on the ordinate. The dimensionless quantity $\gamma\alpha/(2\pi)$ values are plotted on the abscissa. The inset in the figure field shows a change in the $Z_{el}(\omega)$ modulus in the vicinity of the electromechanical resonance frequency.

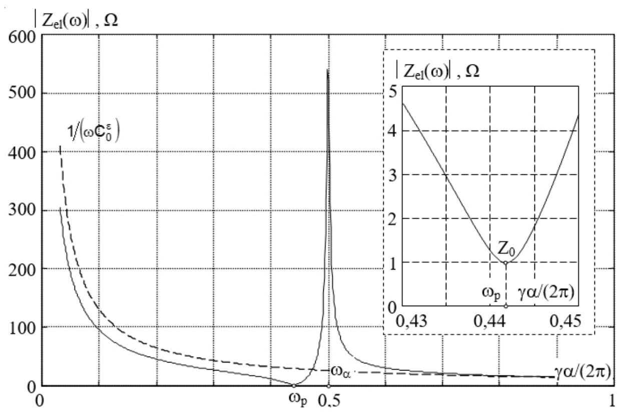

Fig. 3. Graphs for the electrical impedance modulus of the PZT-19 piezoceramic disc, calculated with (solid curve) and without (dashed curve) piezoelectric effect

It follows from the above report that the numerical values of the resonance and antiresonance frequencies are determined by the values of the piezoceramic material constants. From this obvious fact follows the possibility of solving the inverse problem, that is, determining the measured values of the electromechanical resonance frequencies and antiresonance by recalculating the values of the piezoceramic material constants. This possibility determines the relevance and practical significance of mathematical modeling and the subsequent experimental study of oscillating piezoceramic elements and their electrical impedance.

Suppose that for the disk under study, an experimental determination of the frequency-dependent change in the electrical impedance modulus $Z_{el}(\omega)$ in a wide frequency range is performed and a graph similar to that shown in Figure 3 is performed.

We consider the following values to be experimentally determined:

– disc dimensions α, R, in meters;

– disc mass m, in kilograms;

– frequencies of the first resonance f_r and the first antiresonance f_α in hertz, measured to the nearest hertz;

– electrical impedance modulus Z_0 at the frequency of the first electromechanical resonance, in ohms;

– electrical impedance modulus $Z_{el}(\omega_n)$, measured in ohms at low frequency f_n, where $f_n \ll f_r^{(p)}$, where $f_r^{(p)}$ is the frequency of the first radial resonance, whereas $f_r^{(p)} \cong f_r/20$.

The first step will be to determine the density of the piezoceramics $\rho_0 = m/\left(\pi\alpha R^2\right)$. The known value $Z_{el}(\omega_n)$ serves to determine the dynamic electric capacitance of the disc $C_0^\sigma = 1/[2\pi f_n Z_{el}(\omega_n)]$. In this case we naturally assume that $\Lambda_0 \approx 1$. The dielectric constant is determined from the known capacitance $\chi_{33}^\sigma = \alpha C_{33}^\sigma/\left(\pi R^2\right)$.

The f_α frequency of the electromechanical antiresonance satisfies the condition $\pi f_\alpha \alpha/v^D = \pi/2$, where $v^D = \sqrt{{}^0c_{33}^D/\rho_0}$ is the propagation velocity of elastic perturbations of compression – tension in the disk material. The condition noted above determines the velocity v^D and, consequently, the elasticity modulus ${}^0c_{33}^D = (2f_\alpha\alpha)^2\rho_0$. At the resonance frequency $\gamma_r\alpha/2 = \pi f_r\alpha/v^D = \pi f_r/(2f_\alpha)$ the condition results in the following notation for the electromechanical resonance

$$1 - \frac{K_3^2}{1+K_3^2}\cdot\frac{tg\,[\pi f_r/(2f_\alpha)\,]}{[\pi f_r/(2f_\alpha)\,]} = 0,$$

whence

$$K_3^2 = \frac{[\pi f_r/(2f_\alpha)]}{tg\,[\pi f_r/(2f_\alpha)] - [\pi f_r/(2f_\alpha)]}. \tag{32}$$

The known values of the squared electromechanical coupling coefficient K_3^2 and dielectric constant χ_{33}^σ define the dielectric constant $\chi_{33}^\varepsilon = \chi_{33}^\sigma/\left(1+K_3^2\right)$. The known values ${}^0c_{33}^D$ and K_3^2 define the elastic modulus ${}^0c_{33}^E = {}^0c_{33}^D/\left(1+K_3^2\right)$. Since $K_3^2 = e_{33}^2/\left({}^0c_{33}^E\chi_{33}^\varepsilon\right)$, the piezoelectric modulus is determined as $e_{33} = K_3\sqrt{{}^0c_{33}^E\chi_{33}^\varepsilon}$. From the formula (31) it follows that

$$Q_0 = \frac{K_3^2\{[\pi f_r/(2f_\alpha)] - \sin[\pi f_r/(2f_\alpha)]\cos[\pi f_r/(2f_\alpha)]\}}{4(1+K_3^2)\,Z_0\left[(\pi f_r)^2/(2f_\alpha)\right]\,C_0^\varepsilon\cos^2[\pi f_r/(2f_\alpha)]}.$$

Thus, the results of measuring the electromechanical resonance and antiresonance frequencies in the mode of thickness oscillations allow us to establish the numerical values of the elastic modulus ${}^0c_{33}^E$, piezoelectric modulus e_{33}, and permittivity χ_{33}^ε. Quite apart from that, the measured value of the electrical impedance at the resonance frequency can determine the quality factor of the piezoceramics at this frequency.

Measuring the electrical impedance of a piezoceramic disk in a low-frequency range or in the mode of radial oscillations significantly expands the range of experimentally determined piezoceramic physical and mechanical parameters.

Conclusions

This project was undertaken to design an algorithm for assembling and solving a mathematical model of piezoelectric disc transducers, as a result of which the dependences of a piezoceramic disc's electrical impedance on the cyclic frequency have been obtained. Geometric, mechanical, and electrical parameters of these transducers have also been established.

Analytical dependences were obtained, according to which the electrical impedance, the quality factor and amplitude values of the electric charge and electric current on the electroded surfaces of a piezoceramic disc can be determined, provided that the reverse piezoelectric effect is observed. This enabled us to conduct a complete calculation of the problem of a piezoelectric disk's harmonic radial oscillations, by which we have significantly expanded the set of physical and mechanical parameters of piezoelectric ceramics, that, as a rule, are determined experimentally.

The study has revealed the dependence of the change in electrical impedance which significantly depends on the change in the function Λ_0, which, in its turn, depends on the value of the electromechanical coupling coefficient, the wave number of elastic oscillations, and the Voigt indices. The analysis has demonstrated that an increase in the value of $\gamma\alpha/\pi$ from 0 to 1 results in a sharp decrease of Λ_0 from 0,66 down to -2,0. The authors have also determined that at the resonance frequency ω_r ($\Lambda_0 = 0{,}5$), the oscillating piezoelectric disc consumes the maximum possible amount of energy from the electric signal generator.

The comparative analysis of the electric impedance modules obtained with and without consideration of the piezoelectric effect in the disc made of PZT-19 piezoelectric ceramics demonstrated a high coinciding in these data (the difference between the impedance values in these cases did not exceed 18%).

The proposed paper presents the results obtained during the experimental scientific and technical project "Developing a highly efficient mobile ultrasonic system to intensify the extraction process while manufacturing concentrated functional beverages for combatants", that is being implemented by the authors (state registration entry number: 0121U109660, entry date: 12.03.2021).

References

[1] Jim Tran. These Piezo Technologies are Transforming 2022. *ElectronicDesign*, date of access: 08.04.2022.

[2] Aldahiry D. A., Bajaba D. A., Basalamah N. M., Ahmed M. M. (2022). Piezoelectric Transducer as an Energy Harvester: A Review. *YJES*, Vol. 19, Iss. 1, pp. 30–35. DOI:10.53370/001c.33771.

[3] Compamed and Electronica 2022: PI Ceramic Presents Piezo Elements for Medical Technology and the Electronics Industry. *PI Ceramic – Piezo Technology, Actuators & Components*, date of access: 24.10.2022.

[4] Piezoelectric Ceramics Manufacturing Technology. *Ferroperm Piezoceramics*, date of access: 18.10.2022.

[5] Lupeiko T. G., Lopatin S. S. (2004). Old and New Problems in Piezoelectric Materials Research and Materials with High Hydrostatic Sensitivity. *Inorganic Materials*, Vol. 40, Iss. 1, pp. 19–32. DOI:10.1023/B:INMA.0000036326.98414.3c.

[6] Sharapov V., Sotula Z., Kunickaya L. (2014). Piezo-Electric Electro-Acoustic Transducers. *Springer Cham*, 230 p. DOI:10.1007/978-3-319-01198-1.

[7] Huang Y. H., Yen C. Y. (2017). Holographic determination of solid-liquid coupled vibration on development of circular piezoelectric hydrodevices. *15th Asia Pacific Conference for Non-Destructive Testing (APCNDT2017)*, Singapore, ID138.

[8] Mieczkowski G., Borawski A., Szpica D. (2020). Static Electromechanical Characteristic of a Three-Layer Circular Piezoelectric Transducer. *Sensors*, Vol. 20, Iss. 1, 222. DOI:10.3390/s20010222.

[9] Abidin N. A. K. Z., Nayan N. M., Azizan M. M., et al. (2020). The simulation analysis of piezoelectric transducer with multi-array configuration. *Journal of Physics: Conference Series*, Vol. 1432, 012042. DOI:10.1088/1742-6596/1432/1/012042.

[10] Bazilo C., Zagorskis A., Petrishchev O., Bondarenko Y., Zaika V., Petrushko Y. (2017). Modelling of Piezoelectric Transducers for Environmental Monitoring. *10th International Conference "Environmental Engineering"*, Vilnius Gediminas Technical University, Lithuania. DOI:10.3846/enviro.2017.008.

[11] Bazilo C. V. (2017). Principles of electrical impedance calculating of oscillating piezoceramic disk in the area of medium frequencies. *Radio Electronics, Computer Science, Control*, No. 4, pp. 15–25. DOI:10.15588/1607-3274-2017-4-2.

[12] Yanchevskiy I. V. (2011). Minimizing deflections of round electroelastic bimorph plate under impulsive loading. *Problems of computational mechanics and strength of structures*, Iss. 16. pp. 303–313.

[13] Buchacz A., Placzek M., Wrobel A. (2014). Modelling of passive vibration damping using piezoelectric transducers – the mathematical model. *Eksploatacja i Niezawodnosc — Maintenance and reliability*, Vol. 16, Iss. 2, pp. 301–306.

[14] Bazilo C. (2020). Modelling of Bimorph Piezoelectric Elements for Biomedical Devices. In: Hu Z., Petoukhov S., He M. (eds). Advances in Artificial Systems for Medicine and Education III. Advances in Intelligent Systems and Computing. *Springer, Cham*, Vol. 1126, pp. 151–160. DOI:10.1007/978-3-030-39162-1_14.

[15] Wang, Q., Zhao, L., Yang, T., et al. (2021). A Mathematical Model of a Piezoelectric Micro- Machined Hydrophone With Simulation and Experimental Validation. *IEEE Sensors Journal*, Vol. 21, Iss. 12, pp. 13364-13372. DOI:10.1109/JSEN.2021.3070396.

[16] Imperiale S., Joly P. (2012). Mathematical and numerical modelling of piezoelectric sensors. *ESAIM: Mathematical Modelling and Numerical Analysis*, Vol. 46, Iss. 4, pp. 875–909. DOI:10.1051/m2an/2011070.

[17] Jawaid H., Qureshi W. A., Pasha R. A., Malik R. A. (2019). Characterization and Mathematical Modelling of Geometric Effects on Piezoelectric Actuators. *Integrated Ferroelectrics*, Vol. 201, Iss. 1, pp. 201–217, DOI:10.1080/10584587.2019.1668704.

[18] Sofonea M. and Matea A. (2012). *Mathematical Models in Contact Mechanics.* Cambridge University Press, 280 p.

[19] Antonyuk V. S., Bondarenko M. O., Bondarenko Y. Y. (2012). Studies of thin wear-resistant carbon coatings and structures formed by thermal evaporation in a vacuum on piezoceramic materials. *Journal of Superhard Materials*, Vol. 34, pp. 248–255. DOI:10.3103/S1063457612040065.

[20] Sanchez-Rojas J. L. (Ed.). (2020). *Piezoelectric Transducers: Materials, Devices and Applications.* MDPI, University of Castilla-La Mancha, 524 p. doi:10.3390/books978-3-03936-857-0.

[21] Paltanea V., Paltanea G., Popovici D. (2014). Analysis of the Stress-Strain State in Single Overlap Joints Using Piezo-Ceramic Actuators. *7th International Conference on Times of Polymers and Composites (TOP)*, Vol. 1599, pp. 370-373. DOI: 10.1063/1.4876855.

[22] Lin Shuyu, Jie Xu. (2017). Effect of the Matching Circuit on the Electromechanical Characteristics of Sandwiched Piezoelectric Transducers. *Sensors*, Vol. 17, Iss. 2, pp. 329–343. DOI:10.3390/s17020329.

Математичне моделювання дискових п'єзоелектричних перетворювачів для акустоелектронних пристроїв

Базіло К. В., Бондаренко М. О., Усик Л. М., Фауре Е. В., Коваленко Ю. І.

В матеріалах статті представлено алгоритм побудови та дослідження математичних моделей дискових п'єзоелектричних перетворювачів, що знаходять широке застосування в гідроакустиці, мікроелектроніці, мікросхемотехніці (наприклад, як компоненти приймальних антен приладів гідроакустичного зв'язку). Переваги розроблених в статті моделей полягають у можливості встановлення за їх допомогою залежностей, які є математичним описом електроакустичного зв'язку між хвильовими полями на різних ділянках п'єзоелектричного перетворювача дискової форми.

Отримані шляхом математичного моделювання аналітичні залежності дозволяють розрахувати значення електричного імпедансу та добротності разом з амплітудними значеннями електричного заряду та струму на електродованих поверхнях п'єзоелектричного диску за умов зворотного п'єзоелектричного ефекту. Проведений повний розрахунок задачі щодо гармонійних радіальних коливань дискових п'єзоелектричних перетворювачів дозволив суттєво розширити перелік фізико-механічних параметрів п'єзоматеріалу, які раніше визначалися експериментально.

Показана залежність зміни електричного імпедансу від значень коефіцієнту електромеханічного зв'язку, хвильового числа пружних коливань та індексів Фойгта. Також встановлена висока збіжність між модулями електричного імпедансу дисків з п'єзоелектричної кераміки сорту ЦТС (цирконат-титанат свинцю), як з урахуванням, так і без урахування п'єзоелектричного ефекту (розбіжність між значеннями імпедансу в цих випадках не перевищувала 18%).

Ключові слова: п'єзоелектричний перетворювач; акустоелектроніка; математична модель; імпеданс; дисковий елемент